Journal of Power Sources 372 (2017) 134–144

Contents lists available at ScienceDirect

Journal of Power Sources

journal homepage: www.elsevier.com/locate/jpowsour

Impact of operating conditions on the acetylene contamination in the cathode of proton exchange membrane fuel cells

Yunfeng Zhai*, Jean St-Pierre

Hawaii Natural Energy Institute, University of Hawaii–Manoa, Honolulu, HI 96822, USA

HIGHLIGHTS

- Higher acetylene concentration decrease cell performance more.
- Acetylene contamination at higher current density decrease cell performance more.
- Acetylene contamination at lower cell temperature decreases cell performance more.
- Concentration/potential barriers exist, determine tolerance of PEMFC to acetylene.
- Adjusting operation parameters may mitigate acetylene contamination effects.

ARTICLE INFO

Keywords:
Proton exchange membrane fuel cells
Acetylene contamination
Performance degradation
Performance recovery
Operating conditions
Electrochemical impedance spectroscopy

ABSTRACT

Realistically, proton exchange membrane fuel cells (PEMFCs) are operated under varying operating conditions that potentially impact the acetylene contamination reactions. In this paper, the effects of the cell operating conditions on the acetylene contamination in PEMFCs are investigated under different current densities and temperatures with different acetylene concentrations in the cathode. Electrochemical impedance spectroscopy is applied during the constant-current operation to analyze the impacts of the operating conditions on the acetylene electrochemical reactions. The experimental results indicate that higher acetylene concentrations, higher current densities and lower cell temperatures decrease the cell performance more. In particular, cathode poisoning becomes more severe at medium cell current densities. The cell cathode potentials at such current densities are not sufficient to completely oxidize the intermediate or sufficiently low to completely reduce the adsorbed acetylene. Based on these investigations, the possible condition-dependent limitations of the acetylene concentration and cell operating voltage are proposed for insight into the acetylene contamination mitigation stratagem. Regarding the barrier conditions, the acetylene reactions change abruptly, and adjusting the cell operation parameters to change the acetylene adsorbate and intermediate accumulation conditions to induce complete oxidation or reduction conditions may mitigate the severe acetylene contamination effects on PEMFCs.

1. Introduction

In the past few decades, PEMFCs have been considered as one of the most promising clean energy technologies and suitable primary power sources [1,2]. Unfortunately, there are over 200 airborne pollutants that can be introduced into the cathodes of the cells during air feeding. The Pt cathode catalyst for the oxygen reduction reaction (ORR) is sensitive to most of these pollutants, which can adsorb and react on the Pt surface and inhibit the ORRs [3–5]. In other words, most airborne pollutants are potential contaminants for PEMFCs and bring considerable challenges for fuel cell applications.

Recently, a few toxic pollutants, such as NOx, SO_2, halogens and certain volatile organic compounds (VOCs), have been investigated as cathode contaminants in PEMFCs. The results have disclosed the negative impacts of these pollutants on the performance and durability of PEMFCs [6–19]. Since 2010, twenty-one potential contaminants were selected in our group for a PEMFC accelerated contamination study [3,20]. Most of the selected contaminants significantly impacted the cell performance [20]. Acetylene, representing the alkyne airborne contaminants, is one of the critical contaminants that causes more than 50% loss in the cell performance at 45 °C with a concentration of 20 ppm [20]. Acetylene is a widely used welding fuel and chemical synthesis reagent. The acetylene concentration near a production plant estimated by a diffusion model is 5.5 (1 h average) and 3 (24 h average)

* Corresponding author.
E-mail address: yunfeng@hawaii.edu (Y. Zhai).

http://dx.doi.org/10.1016/j.jpowsour.2017.10.072
Received 23 June 2017; Received in revised form 20 October 2017; Accepted 21 October 2017

ppm by volume [21].

Acetylene contamination mechanisms in PEMFCs have been developed using in situ and ex situ gases and electrochemical analyses [22–24]. Acetylene adsorbs on PEMFC electrodes and inhibits ORRs in the cathode. At cathode potentials above 0.65 V, adsorbed acetylene is electro-oxidized into carbon dioxide and desorbs easily [24]. At potentials below 0.3 V, adsorbed acetylene is reduced to ethylene, ethane and methane, and the reduction products desorb even more rapidly. However, when cells are operated with cathode potentials between 0.65 V and 0.3 V, the electro-oxidation intermediate CO (or COH-type species) forms above 0.5 V, and the electroreduction intermediates vinylidene and ethylidyne form below 0.3 V. Those intermediates are stable during electro-oxidation, especially vinylidene and ethylidyne, and accumulate on the cathode, significantly depressing ORRs. These reaction mechanisms suggest that the acetylene contamination process in PEMFCs probably strongly depends on the operating conditions.

As a candidate power source, PEMFCs have been operated at varying operating conditions. From a previous investigation of SO_2 contamination in PEMFCs, the concentrations of the contaminants, cell current density and temperature were determined to be important operating parameters that can affect SO_2 contamination significantly [25]. Therefore, in this paper, the cell performance responses to acetylene exposure were investigated under different cell current densities and temperatures with different acetylene concentrations. Electrochemical impedance spectroscopy (EIS) and Polarization (VI) curves were analyzed to understand the effects of the operating conditions on the acetylene contamination in the PEMFCs. Furthermore, the cell performance recovery and mitigation strategies were proposed for various cell operation conditions.

2. Experimental

The acetylene contamination experiments were conducted on an FCATS™ G050 series test station (Green Light Power Technologies Inc.) with an internal 50 cm^2 single cell and an anode/cathode flow field with double/triple serpentine channels [22,24]. Gore PRIMEA M715 catalyst-coated membranes (MEAs) were used for all acetylene contamination tests. The catalysts were 50% Pt/C, with a Pt loading of 0.4 mg Pt cm^{-2} on each side of the MEA. The MEAs were assembled between the two flow fields with 25 BC gas diffusion layers (GDL, SGL Tech.).

After the full activation and diagnostics procedures were conducted before contamination testing (BOT) with a new MEA [22], an acetylene contamination experiment was conducted under the operating conditions listed in Table 1. The operating conditions at the anode/cathode were as follows: 100/50% relative humidity (RH) and a 2/2 flow stoichiometry; and the outlet back pressures were 48.3/48.3, 10/10, and 5/5 kPa g for cell temperatures of 80 °C, 45 °C, and 10 °C, respectively, which corresponded to the pressure of the dry reactants in the cell chamber at 1 atm. Acetylene concentrations were larger than in ambient air to accelerate tests and facilitate the separation of degradation effects. Each contamination experiment included three phases of constant-current operation (CCO): (i) pre-poisoning with neat air, (ii) poisoning until a steady cell performance was achieved, and (iii) self-induced performance recovery with neat air until a steady performance was reached. The gas mixtures were supplied by Matheson Tri-Gas Inc. and contained 20, 100, 400 or 4000 ppm acetylene by volume in air. Before and after the CCO procedure, the VI curves were measured from the high current to the open-circuit voltage (OCV) with a stabilizing time of 15 min at each current set point under operating conditions similar to those of the constant-current (CCO) operation.

Table 1
The operating conditions matrix for the constant-current contamination experiments with acetylene in the PEMFC cathode.

Test ID	Acetylene Concentration [ppm]	Current Density [A cm^{-2}]	Temperature [°C]
1	20	1	80
2	50	1	80
3	100	1	80
4	200	1	80
5	300	1	80
6	400	1	80
7	500	1	80
8	5	1	45
9	20	1	45
10	100	1	45
11	100	0.2	80
12	100	0.6	80
13	200	1.5	80
14	300	0.2	80
15	300	0.6	80
16	100	1	10

During CCO procedure, AC impedance data were obtained from 0.1 Hz to 10 kHz (10 points per decade) using a Solartron SI1260 Impedance/Gain-Phase Analyzer and Stanford Research SR560 Low Noise Preamplifiers with ZPlot® (Scribner Associates) software. An AC current perturbation resulting in a voltage change of approximately 5 mV, was applied on the single cell during CCO at a DC current of 75, 50, 30 or 10 A.

3. Results and discussion

3.1. Cell performance degradation and recovery

3.1.1. Acetylene concentration effect

The concentration effect on the acetylene contamination in PEMFCs was investigated using three-phase constant-current experiments with a current density of 1 A cm^{-2}. Fig. 1 a) and b) show the cell voltage response to acetylene with different concentrations at 80 and 45 °C, respectively. It should be noted that the cell voltage responses to 20, 50 and 100 ppm acetylene were similar, and those to 400 and 500 ppm acetylene were similar. Therefore, the results of tests 1, 2 and 6 in Table 1 are not shown in Fig. 1 a). It can be seen that all cell voltages dropped immediately within the first several minutes of acetylene exposure. However, the following responses were significantly different for each concentration, especially the cell operated at 45 °C, though all MEAs reached stable performance during the first 5 h of operation with neat H_2/Air.

For the cells tested at 80 °C, when the acetylene concentration was lower than a certain value, the cell voltage degradation showed similar behaviors. The exposure to 100 ppm acetylene is discussed as an example. The cell voltage dropped ~40 mV, from 0.672 V to 0.635 V, during the first minute, increased ~20 mV up to 0.653 V within the second minute, then reached to a stable voltage of 0.663 V during the following 30 min. At the poisoning equilibrium state, the 100 ppm acetylene caused a total loss of ~10 mV in the cell voltage. Within ~3 min after the acetylene injection was stopped, the cell voltage of both cells recovered to its initial value before exposure. When the acetylene concentration was higher than 300 ppm, the cell voltage degradation showed different behaviors from those observed at a low concentration. For the exposure to 300 ppm acetylene, two stages were involved in the degradation of the cell voltage. At the beginning of the exposure, the cell voltage dropped approximately 20 mV, from 0.677 to 0.653 V within 2 min. Next, slow transient degradation was observed, followed by a second rapid decrease. After approximately 30 min of exposure, the cell voltage decreased to 0.110 V, and the degradation slowed down again. At approximately 1 h of acetylene exposure (6 h into the experiment), the cell voltage reached a steady value of approximately 0.082 V. This final poisoned state represented an approximately 88% loss in the cell performance. When the acetylene injection was stopped, the cell voltage increased immediately. The cell voltage recovery also included two stages, and these two stages of

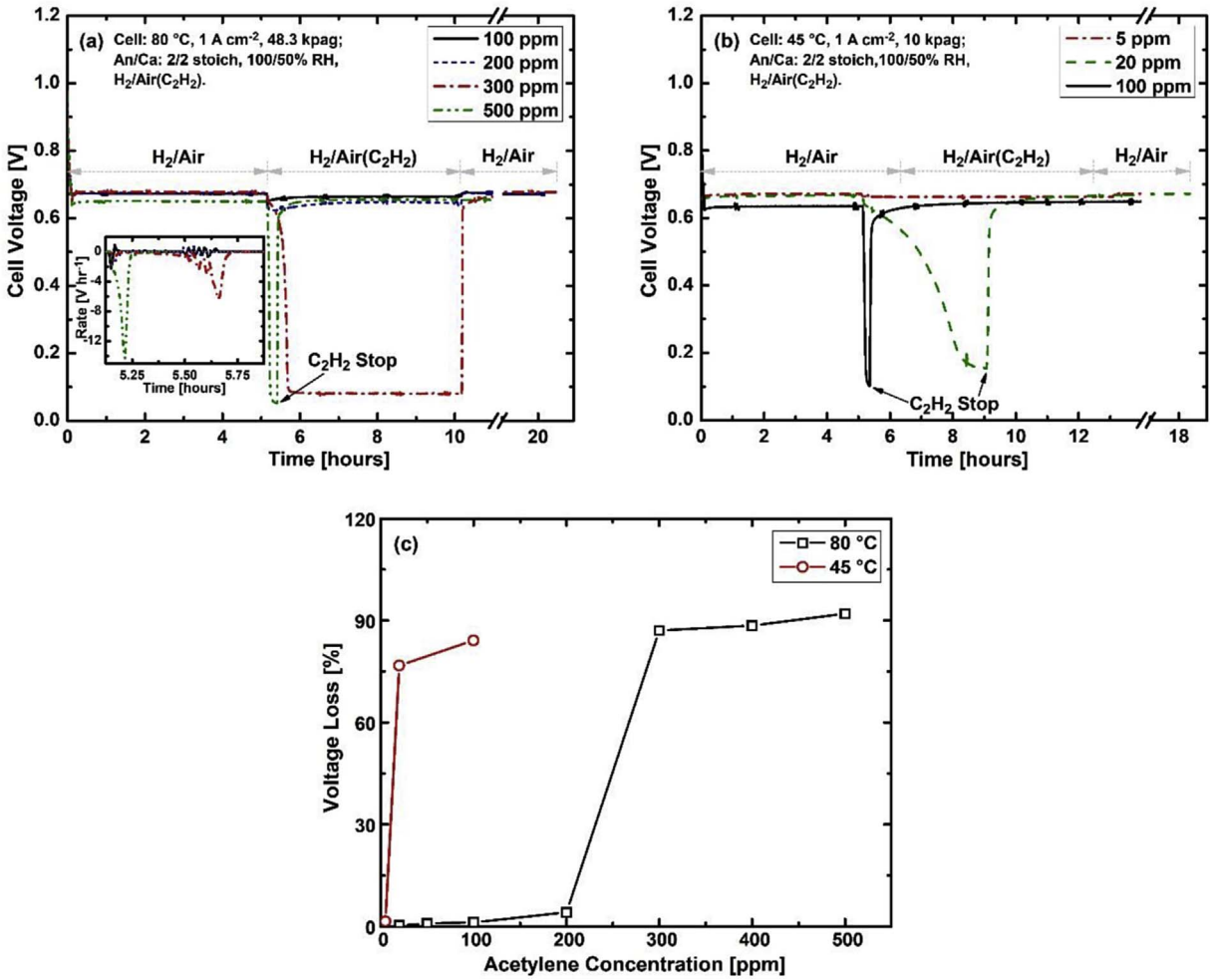

Fig. 1. Cell performance response to acetylene in the air stream of a PEMFC with different concentrations at: a) 80 °C and b) 45 °C; and c) a summary of the cell performance losses with different acetylene concentrations. (For interpretation of the references to colour in this figure legend, the reader is referred to the web version of this article.)

recovery corresponded to the two stages of degradation. Within the first minutes of recovery, the cell voltage increased to 0.639 V, restoring over 94% of the original cell performance. Then, the voltage recovery slowed down. After approximately 3 h of operation with neat air, the voltage reached the initial value of 0.677 V. For the 500 ppm acetylene exposure, at approximately 15 min, the exposure was stopped due to the low cell voltage reaching the low limit value of the test station. The cell voltage recovery also exhibited two stages that were the same as those after contamination with 300 ppm acetylene.

To illustrate and compare the cell voltage degradation behaviors, the cell voltage variation rates (the derivative of the cell voltage over time, $\partial V/\partial t$; negative values indicate degradation) during the first hour of acetylene exposure are shown in the inset of Fig. 1 a) as examples. The peaks in the voltage curves from 5.45 to 5.6 h were attributed to the contributions of AC impedance perturbations but not the acetylene contamination. Corresponding to the low and high acetylene concentrations, the cell voltage degradation rate exhibited one peak and two peaks, respectively. For instance, for the cells exposed to 100 ppm acetylene, the cell voltage degradation rate exhibited one peak at ~5.15 with values of -2.24 V h^{-1}. For the cell exposed to 300 ppm acetylene, the cell voltage degradation rate exhibited two peaks at ~5.17 and ~5.66 h with values of -1.27 and -6.38 V h^{-1}, respectively. A minimum voltage degradation rate of -0.12 V h^{-1} at ~5.27 h exhibited an inflection point between the two peaks, which divided the cell voltage degradation curve into two stages. The cell voltage at the inflection point was approximately 0.637 V. For the cell exposed to 500 ppm, only one significant degradation rate peak at ~5.22 h with a value of -14.34 V h^{-1} was observed, with an obvious shoulder at ~5.16 h. The degradation rate of the 500 ppm acetylene test was approximately 10 times that of the first degradation stage at other concentrations.

For cells tested at 45 °C, similar behaviors as those at 80 °C were observed. A concentration of 5 ppm acetylene in the cathode slightly affected the cell performance, but 20 ppm acetylene significantly degraded the cell voltage. The cell performance loss during 5 ppm acetylene exposure was ~10 mV, less than 1.5%. However, that with 20 ppm acetylene reached 80% within the two stages of cell voltage degradation. The two stages in the voltage degradation curve of the 20 ppm acetylene test were clearly indicated by the inflection point at ~0.63 V. For the 100 ppm acetylene exposure, the cell voltage showed one rapid degradation stage and two recovery stages, the same features as those of the 500 ppm acetylene test at 80 °C. Within ~5 min, the cell voltage dramatically decreased to ~0.480 V, from 0.635 to 0.152 V. Then, the degradation slowed down and reached a relative steady state with a value of 0.100 V at approximately 15 min of exposure. The exposure was stopped due to the low cell voltage. The two stages of the cell voltage recovery included the following: within the first 3 min, the voltage jumped up to 0.550 V, restoring over 87% of the original cell performance; after approximately 2 h, the voltage was then restored to the initial value. However, the cell voltage continually increased until reaching a stable value of 0.648 V after ~8 h of recovery, which exceeded 13 mV over the initial cell performance.

As discussed in the previous work, the adsorption/reactions of acetylene on Pt surfaces are dependent on the applied potential and

competition with the ORR when the cathode is exposed to acetylene [22]. During exposure to 100 and 200 ppm acetylene at 80 °C and 5 ppm acetylene at 45 °C, the cell cathode potentials were sufficiently high (voltages higher than 0.64 V) to completely oxidize acetylene and the oxidation intermediates (COH-type intermediates and CO) and there was no adsorbate accumulation on the electrode. The cell performance losses in the steady poisoning state in Fig. 1 a) and b) were attributed to the chemical reactions between the acetylene and oxygen and the electro-oxidation of acetylene on the Pt surface, which competed with the ORR and reached stable coverage on the Pt surface. The slightly voltage increases observed before reaching the steady poisoning state were attributed to the redistribution of the cell current [26]. The inlet part of the cathode was contaminated earlier and more severely than the outlet, which was a result of the acetylene concentration gradient along the inlet toward the outlet due to the geometric effect. As soon as acetylene feeding was stopped, the adsorbates on the Pt surface were oxidized immediately and completely. The poisoned Pt sites were then cleaned and once again available for the ORR, restoring cell performance to the initial value. With higher concentrations of acetylene, such as 300 ppm and above at 80 °C and 20 ppm and above at 45 °C, the competition between the acetylene oxidation on the Pt surface with the ORR immediately caused a slightly higher cell performance loss, such as that during the first stage of degradation. However, the acetylene oxidation produced more CO- and COH-type intermediates, and the electro-oxidation of those intermediates on the Pt surfaces was slow at pre-peak potentials [27,28]. The cathode potential after the first stage was not sufficiently high to completely oxidize all of the produced intermediates that would accumulate on the Pt surface. The accumulation of the intermediates inhibited the ORR and increased the ORR overpotential at the cathode, decreasing the cell voltage. The slow voltage decrease during the transient period was a result of the initial accumulation of CO and COH intermediates on the Pt surface, which facilitated further accumulation of the intermediates. The accumulation of intermediates and the degradation of the cell voltage were coordinated with and promoted each other, as shown in the degradation rate curve before the second peak. The second rapid drop in the cell voltage subsequently occurred, creating the second degradation rate peak. When the cathode voltage was decreased to a certain value, for example the cell voltage at 0.23 V for 80 °C and at 0.28 V for 45 °C according to the second voltage degradation rate peaks, the oxidation of acetylene and accumulation of the intermediates slowed down, which resulted in slower degradation of the cell voltage. When the cell voltage reached a lower value, such as 0.15 V, the adsorbed acetylene was readily electroreduced to ethylene and ethane, which was easily desorbed [24,29,30]. The steady poisoning state at the low cell voltage occurred due to the competition between and combination of acetylene reduction and the ORR equilibrium with a certain coverage of intermediate residues on the Pt surface. Slight differences were observed among the onset voltages and steady poisoning state voltages between the tests at 80 °C and 45 °C, which were attributed to the temperature and feeding concentration effect on the oxidation and reduction of acetylene. Regarding the tests with 500 ppm acetylene at 80 °C and 100 ppm acetylene at 45 °C, the higher concentration resulted in a faster production of intermediates, resulting in very rapid cell voltage degradation, earlier acetylene reduction and ORR equilibrium. The higher concentration also increased the competition of the acetylene reduction on the Pt surface, resulting in lower steady poisoning state voltages. For all tests involving the second stage of voltage degradation, the adsorbed acetylene could desorb and continuously be reduced, exposing most of the Pt sites to the ORR reaction after the acetylene injection was completed. This release corresponded to the first stage of voltage recovery. However, a few CO and COH intermediates remained on the Pt surface, and these intermediates must have been oxidized and/or desorbed slowly until intermediates no longer remained in the second recovery stage during several hours of operation with neat air. The 13 mV excess recovery after the 100 ppm acetylene test at 45 °C may have been due to the modification on the interface between the electrolyte film and Pt/C surface induced by the acetylene reaction on the Pt surface, which will be discussed in the EIS analysis section.

The concentration effects on the acetylene contamination are shown in Fig. 1 c). The dependence of the cell voltage loss on the acetylene concentration comprised three levels: i) at a low concentration level, the cell performance loss increased slowly and linearly with the increase in the acetylene concentration; ii) within 200–300 ppm at 80 °C and 5-20 ppm at 45 °C, an acetylene concentration barrier existed that abruptly triggered cell performance loss; and iii) at a high concentration level, the cell performance loss slowed down and became linearly dependent on the acetylene concentration again. The single cell could be considered as a plug-flow electrochemical reactor for acetylene. The electrochemical and catalytic reaction rates of acetylene positively depended on the acetylene concentration, the effective active area of the electrode and the cell cathode potential. The cell performance loss, i.e., the contamination overpotential, positively depended on the coverage of the acetylene and other intermediate adsorbates on the electrode surface, which increased with the increase in the acetylene concentration. At a low concentration level, the acetylene feeding flow rate was low; the effective active area and potential of the cathode were sufficiently high to completely oxidize all the acetylene into CO_2; the cathode became stabilized at a high potential; and the cell performance loss increased slowly with the increase in the acetylene concentration. When the acetylene concentration was higher than the trigger value, the effective active area and potential of the cathode were no longer sufficiently high to completely oxidize the acetylene into CO_2; the intermediates of acetylene started accumulating on the Pt surface; the contamination overpotential was reached, and the rapid cell performance loss rapidly corresponded to the intermediate accumulation until the cathode potential was no longer sufficient to oxidize the acetylene. At a high acetylene concentration level, the oxidation intermediates of CO and COH accumulated on the Pt surface until reaching saturated coverage; the significant contamination decreased the cathode potential sufficiently to reduce the acetylene completely. All the reactions reached equilibrium again at a low potential, and the increase in the acetylene concentration resulted in increased acetylene coverage, which in turn caused the cell performance loss to increase slowly again.

3.1.2. Cell current density effect

Fig. 2 a) and b) and c) show the cell voltage responses to 100, 200 and 300 ppm acetylene, respectively, under different cell current densities. The cell voltage degradation rates during the first 2 h of acetylene exposure are shown in the insets of Fig. 2 b) and c) for comparing the cell voltage degradation behaviors. When exposed to 100 ppm acetylene, the cell performance of all MEAs at different current densities slightly decreased. The cell voltages at 0.2, 0.6 and 1 A cm^{-2} dropped approximately 15, 22 and 40 mV within 4, 2 and 1 min, respectively, then slowly increased to 5, 12 or 30 mV reaching a stable poisoning state at 0.790, 0.713 and 0.664 V in the following 0.13, 1.5 and 1.5 h, respectively. With the increase in the cell current density, the maximum cell voltage loss increased, and the time to reach the maximum loss decreased. However, regardless of the degradation history and the current density, the final cell voltage losses in the steady poisoning state were approximately the same at 10 mV. When the acetylene injection was stopped, the voltages of all cells recovered to their initial values before exposure within ~3 min.

When exposed to 200 ppm acetylene, the voltage loss at 1 A cm^{-2} was ~30 mV at the poisoning equilibrium state, which was analyzed in section *3.1.1*. However, the cell voltage at 1.5 A cm^{-2} shows an obviously different response; two stages can be observed in the voltage degradation cure, even though they are not clearly separated. A ~30 mV initial drop during 1 min was followed by a significant decrease of 0.5 V within the subsequent ~30 min; then, the decrease slowed down, and the cell voltage reached a relative steady value of

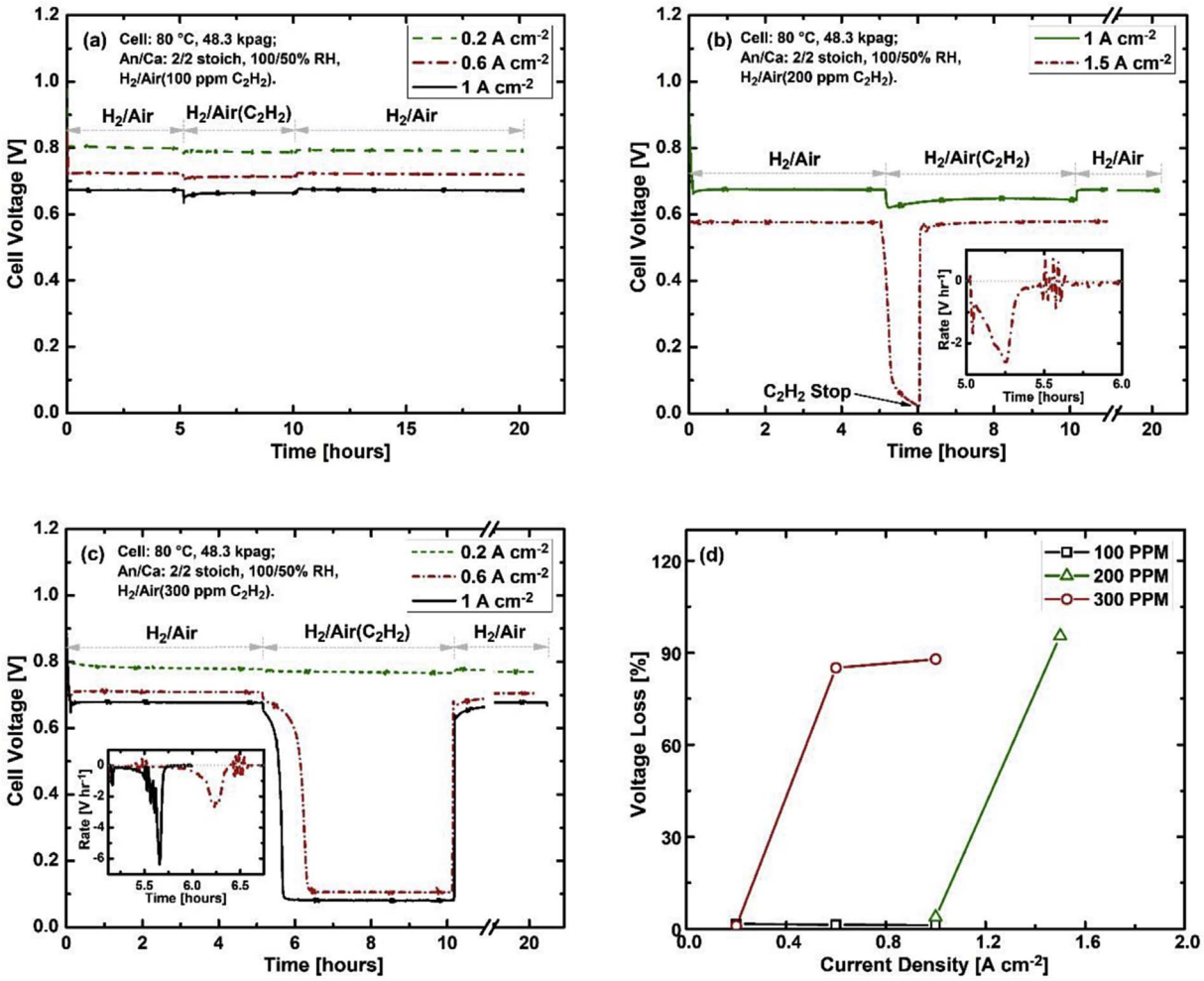

Fig. 2. Cell voltage response to a) 100 ppm, b) 200 ppm and c) 300 ppm acetylene in the air stream of a PEMFC under different operating cell current densities and d) the cell performance loss at different current densities. (For interpretation of the references to colour in this figure legend, the reader is referred to the web version of this article.)

0.02 V at approximately 1 h of exposure. Correspondingly, the two degradation rate peaks were -1.68 and -2.61 V h^{-1} at ~1 and ~30 min of exposure, respectively, as shown in the inset of Fig. 2 b). The cell voltage recovery also included two stages: during 2 min of operation with neat air, the cell voltage increased to 0.550 V, restoring over 95% of the original cell performance; in the following 2 h, the cell voltage slowly recovered to the initial value of 0.576 V.

For the exposure to 300 ppm acetylene, the cell voltage at 0.2 A cm^{-2} only showed a slight decrease during the first 3 min, resulting in a ~10 mV cell voltage loss in the steady poisoning state. The cell voltage also recovered to its initial value within ~3 min after the acetylene injection was stopped. The cell voltage at 0.6 A cm^{-2}, however, shows two stages of degradation, which were similar with those at 1 A cm^{-2} except a clearer transient period existed between the two peaks. The contamination before the transient period was considered as a quasi-steady poisoning state. In the first stage, the cell voltage dropped by ~20 mV to 0.688 V within 2 min. In the second stage, the cell voltage dropped by ~0.580 V–0.105 V within ~1.5 h. The two corresponding peaks in the voltage degradation rate curve are shown in the inset of Fig. 2 c) with values of -0.93 and -2.68 V h^{-1} at ~1 min and ~1.1 h of exposure, respectively. The two stages of voltage recovery included ~95% of the original cell performance in the first 3 min, and the rest occurred during the following ~7 h. The results at 1 A cm^{-2} were already analyzed in section *3.1.1* and are not repeated in this section.

As discussed above, the acetylene reactions on the Pt/C relied on the cathode potential. In particular, for the further oxidation of the CO- and COH-type intermediates, the initial cell voltage should have been higher than 0.64 V at 1 A cm^{-2}. The cell with a low current density had a high initial cell voltage, which was associated with a high cathode potential. The results in Fig. 2 a) can be explained as follows: the acetylene concentration was 100 ppm, lower than the trigger value, and the cathode potential was sufficiently high to completely oxidize the CO- and COH-type intermediates. Intermediates did not accumulate on the Pt surface of the cathode. The control reaction may have been the first step of acetylene oxidation. The oxidation rate and the coverage of acetylene depended on the acetylene concentration. Therefore, in the steady poisoning states, the 100 ppm acetylene in the cathode caused the same cell performance loss, even for the cells at different current densities. However, at the high current density, the acetylene flow rate in the feeding air stream was higher than that at the low current density with the same stoichiometry. The higher feeding rate might have resulted in a faster and more severe current redistribution along the flow channel [26]. In addition, a faster and more severe cell performance loss occurred when the acetylene injection started instantaneously at high current densities, as shown in Fig. 2 a). For the results in Fig. 2 b), in the first degradation stage, the cell at 1.5 A cm^{-2} exhibited a similar voltage loss to that at 1 A cm^{-2}. These performance losses were the result of the concentration-dependent oxidation of acetylene on the Pt surfaces. However, the cell at 1.5 A cm^{-2} had a high acetylene flow rate as well as a low voltage after the first stage of degradation. These disadvantages triggered the accumulation of the CO- and COH-type intermediates on the cathode and the second stage of degradation until the acetylene oxidation started to reduce. These results are also

consistent with the potential-dependent processes during acetylene contamination in the PEMFCs. There are the similar reasons for the 300 ppm acetylene contamination at the different current densities shown in Fig. 2 c). Comparing the voltage degradation curve at 0.6 A cm^{-2} to that at 1 A cm^{-2}, the prolonged second degradation stage suggests the influence of the acetylene flow rate on the degradation; the lower flow rate caused slower accumulation of the CO- and COH-type intermediates on the cathode and a later arrival of the second stage degradation.

The effects of the cell current density on the acetylene contamination are summarized in Fig. 2 d). Generally, the cell voltage and cathode potential decreased with the increase in the current density, as will be discussed in terms of the polarization curves in section *3.3.2*. The changes in the cathode potential in turn affected the acetylene reactions on the cathode. For the MEAs used in this work, the IR voltage (ohmic-polarization-corrected cell voltage) only decreased slightly with the increase in the current density. The IR voltage was still as high as 0.69 V, even when the current reached 2 A cm^{-2}. This indicates that the cell cathode potential was even higher than 0.70 V for all the exposure experiments. From Fig. 2 d), with low concentrations of acetylene, i.e., 100 ppm, the cell performance loss was not obviously affected by the changing current density. Because the cell cathode potential and the effective active area of the electrode were sufficient to completely oxidize the feed acetylene within the inlet region of the flow field, the potential-dependent accumulation of the intermediates was not triggered. However, with high concentrations of acetylene, i.e., 200 and 300 ppm, the effective active area of the electrode was not sufficient to completely oxidize the feed acetylene, and the potential-dependent accumulation of the intermediates was triggered. The cell performance loss increased rapidly when the current density was increased. For example, the current density increased from 1 to 1.5 A cm^{-2} and 0.2–0.6 A cm^{-2} with exposure to 200 and 300 ppm acetylene. When the fast acetylene reduction dominated the acetylene reactions and all reactions reached equilibrium at a low potential, the performance loss depended on the cell current density in the same way as the acetylene concentration at low cell voltage levels. The cell performance loss increased slowly again with the increase in the cell current density because the Pt sites for the oxygen reaction became covered by acetylene, decreasing the reaction rate.

3.1.3. Cell temperature effect

The cell voltage responses to 100 and 20 ppm acetylene at different temperatures are shown in Fig. 3 a) and b), respectively. The initial cell voltage at 10 °C was only ~0.53 V, which was much lower than that at high temperature. For the cell exposure to 100 ppm acetylene, within 1 min, the voltage dropped to 0.160, and in the following 3 min, the voltage reached a relative steady state at 0.05 V. Then, the cell performance started to recover due to the auto termination of acetylene exposure. However, unlike that at high temperatures, the recovery was very slow and included three parts. In the first 30 min, the voltage recovered to ~0.47 V. Then, the recovery became slower, reaching a stable state at ~0.52 V after approximately 8 h; however, ~10 mV could not be restored by the neat air operation. We attempted to recover the irreversible cell performance loss using an OCV operation. After 3 min of maintaining the OCV, the cell performance was restored completely to its initial value. These behaviors are in sharp contrast to the cell responses observed at 80 and 45 °C, which were analyzed in Fig. 1 a). With regard to the exposure to 20 ppm acetylene at 80 °C, the contamination effect only minimally affected the cell performance. The cell voltage dropped by ~20 mV from 0.667 V during the first 3 min and then reached a stable value at 0.663 V. The total loss was only 4 mV. The recovery was completed in neat air. However, the cell response at 45 °C showed two-stage degradation and a severe acetylene contamination effect, as was analyzed in Fig. 1 b).

The effects of the cell temperature on the acetylene contamination are plotted in Fig. 3 c). With the increase in the cell temperature, the cell voltage loss decreased dramatically. Typically, at a high cell temperature, the surface potential on the catalysts was high, and both the catalytic and electrochemical oxidation of acetylene on the Pt surface could be accelerated. Furthermore, at a high cell temperature, the coverage of acetylene and its oxidation intermediates, especially CO, was much lower than that at low cell temperatures. Therefore, the high cell temperature not only improved the acetylene oxidation rate but also inhibited the adsorption of the acetylene oxidation intermediates. As a result, intermediate accumulation on the Pt surface was avoided when the acetylene concentration was less than the trigger value, the second degradation stage was not triggered, and the cell performance response exhibited only a slight contamination effect.

3.2. Electrochemical impedance spectroscopy analysis

3.2.1. Acetylene concentration effect

The impedance spectra obtained during the pre-poisoning and steady states of the acetylene experiments are shown in Fig. 4 a) in the Nyquist plots. The experiments with low concentration acetylene showed similar impedance spectra features, and those with high concentration acetylene showed similar features, as represented by the results of the 200 ppm and 300 ppm experiments, respectively. Before exposure to acetylene, both MEAs exhibited typical EIS behavior at high current densities, which was characterized by three distinguishable depressed semicircles [31]. When the cell cathode was exposed to 200 ppm acetylene, the mid and low frequency arcs of the EIS in the steady poisoning state were slightly expanded compared to the arcs before exposure. These changes indicated that the adsorption and oxidation of acetylene in MEA affected not only the ORR but also the mass transport of the oxygen in the MEA. However, the exposure to 300 ppm acetylene resulted in entirely different EIS features in the steady poisoning state. The mid and low frequency arcs were much larger than those before exposure. In addition, inductive loops at low frequencies were observed, which corresponded to the area of the curve under Im (Z) = 0 in Fig. 4 a). The significantly expanded arcs at mid frequencies indicate that the ORR was severely sluggish, which was a result of ECA loss due to coverage by the acetylene intermediates [31]. The expansion in the arcs at low frequencies is typically attributed to mass transport effects, especially the part of the curve above Im(Z) = 0. For ORRs on Pt surfaces in the absence of contaminants, the inductive loop at low frequencies indicates other reaction mechanisms, which are supposed to originate from the reduction response of ORR intermediates, such as H_2O_2 formed during the ORR at low cathode potentials with a high impurity coverage [31]. For the acetylene contamination case, the reduction of acetylene should be another contributor to the inductive loop, as explained in our previous work [22]. Therefore, the expansion in the arcs at low frequencies might have been a combination of mass transport effects and the reduction responses of the ORR intermediates and acetylene. This inductive response was complicated and will be studied specifically in the future.

The ECM, inset of Fig. 4 a), was applied to analyze the impedance spectra obtained during the contamination experiments. The electronic elements R and L stand for the serial resistance of the proton and electron transport and inductance in the bulk system, respectively, and Ca, Ra and Rc represent the capacitance of the anode double layer and charge transfer resistance of the HOR and ORR, respectively. The constant phase element (CPEc) is associated with the double-layer capacitance of a real cathode with a rough catalyst layer, a non-uniform catalyst distribution, and the finite-length Warburg diffusion element (Wc) with the oxygen diffusion resistance, Rd, in the GDE [31]. It should be noted that this ECM does not include inductive elements in the cathode circuit and is only suitable for EIS without a significant inductive loop at low frequencies, i.e., the responses of low concentrations of acetylene or the responses during the first degradation stage of high concentrations of acetylene contamination. The EIS obtained during the steady poisoning state from the 200 ppm acetylene

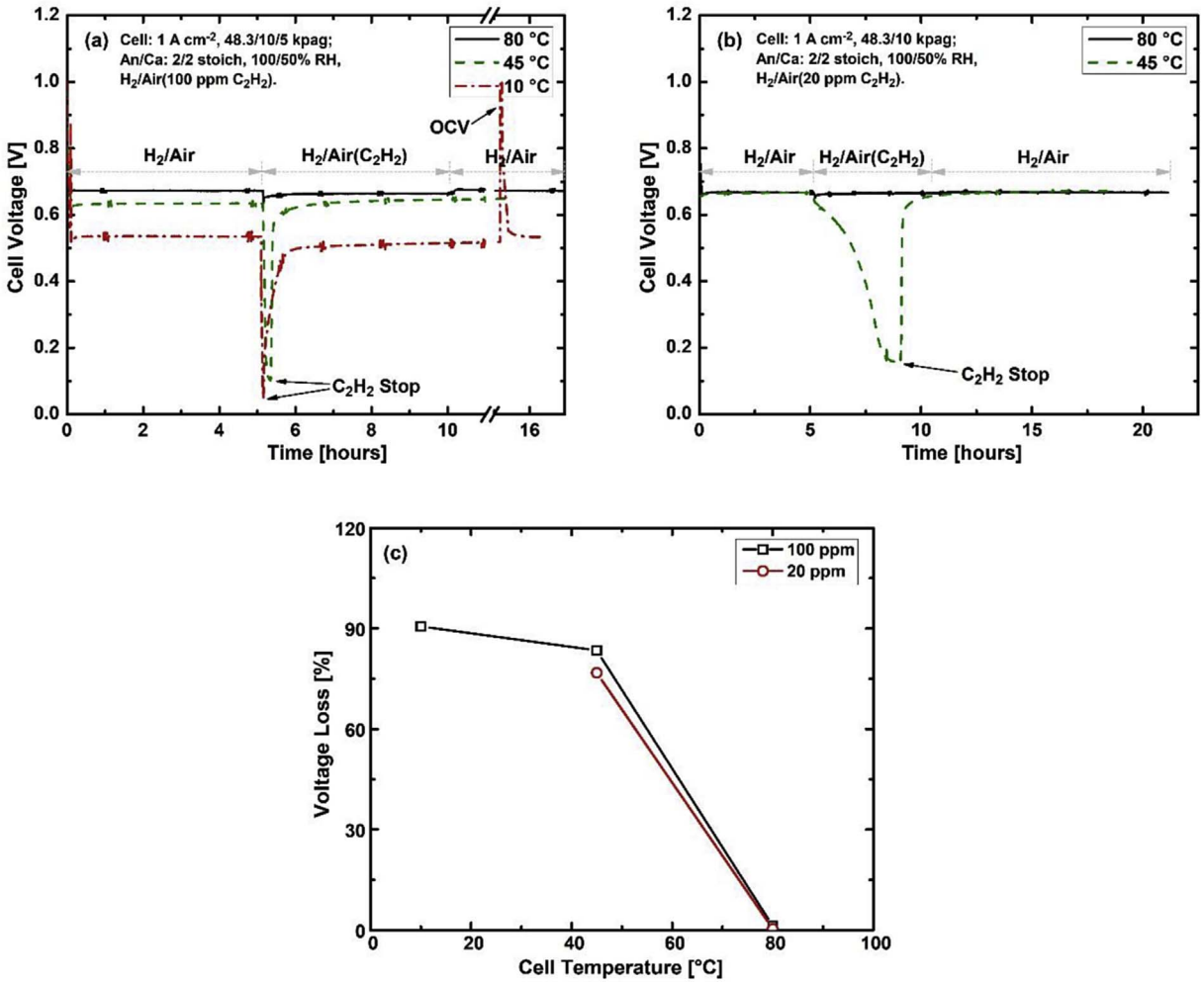

Fig. 3. Cell performance response to a) 100 ppm and b) 20 ppm acetylene in the air stream of a PEMFC under different cell temperatures and c) the cell performance loss at different temperatures. (For interpretation of the references to colour in this figure legend, the reader is referred to the web version of this article.)

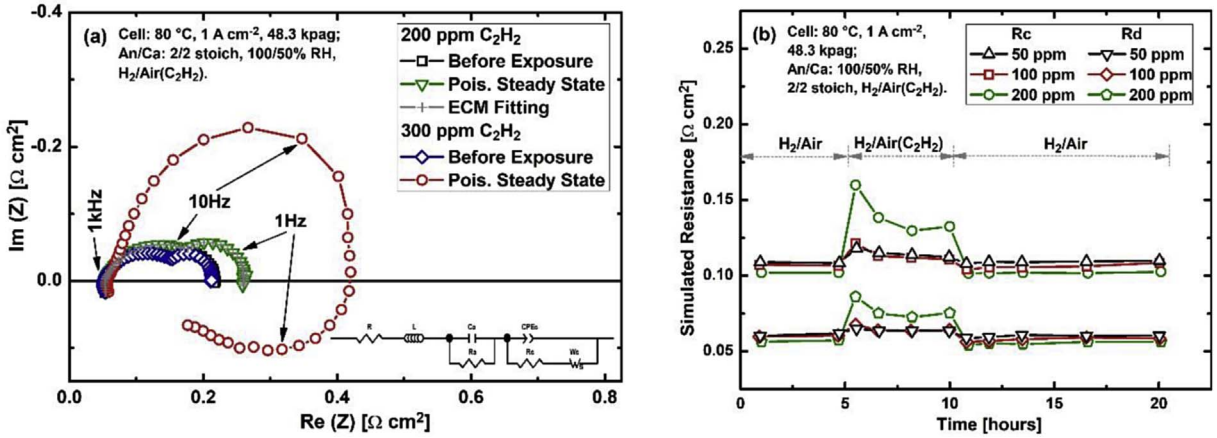

Fig. 4. a) EIS of the MEAs during acetylene contamination experiments with different concentrations and a current of 1 A cm^{-2} at 80 °C (the inset is an ECM used for fitting the EIS). b) The variation in the cathode charge transfer resistance, Rc, and cathode gas diffusion resistance, Rd, during the acetylene contamination experiments. (For interpretation of the references to colour in this figure legend, the reader is referred to the web version of this article.)

experiment were fit using the ECM in Fig. 4 a) to provide an example of an EIS obtained during the acetylene experiments with low concentration. The fitting results are shown in Fig. 4 a) as an example of the labeled ECM fitting, which fits well with the experimental responses over the whole frequency range with a squared error sum of ~1%.

The ECM parameters R, Ra, Rc and Rd were extracted from the ECM simulation for the EIS obtained during the contamination experiments with 50, 100 and 200 ppm acetylene. Obvious changes in R or Ra were not observed throughout the CCO procedure. Therefore, only variations in Rc and Rd during the acetylene contamination experiments are compared in Fig. 4 b). The data from the 50 ppm acetylene test almost overlapped with those of the 100 ppm test. Before exposure, Rc was

constant at approximately 0.109, 0.107 and 0.102 Ω cm^2 and Rd was 0.062, 0.061 and 0.057 Ω cm^2, respectively, for the 50, 100 and 200 ppm acetylene tests. This indicates that all MEAs exhibited similar ORR charge resistances and similar mass transfer resistances. When exposed to acetylene, the MEAs showed similar variation trends in their Rc and Rd values: they increased first and then decreased slightly until reaching steady values. At the steady poisoning state, Rc increased to approximately 0.114, 0.112 and 0.130 Ω cm^2, and Rd increased to 0.064, 0.064 and 0.073 Ω cm^2, respectively, for the 50, 100 and 200 ppm acetylene tests. The increases in Rc and Rd were attributed to the competition between acetylene oxidation on the Pt and the ORR and accounted for the cell performance losses during the acetylene contamination. The slight decreases before reaching the steady state were attributed to the current redistribution along the flow fields [26]. When comparing the changes in Rc and Rd with different acetylene concentrations, the adsorption of 50, 100 and 200 ppm acetylene correspondingly caused a ~4.6%, ~4.7% and 27.5% increase in the Rc and a 3.2%, 4.9% and 28.1% increase in the Rd. Higher concentrations of acetylene caused Rc and Rd to further increase. This result can be explained because higher concentrations of acetylene resulted in more acetylene coverage and reaction competitiveness compared to the ORR on the Pt surface, resulting in an increased ORR resistance. After recovery, both Rc and Rd returned to their initial values for all MEAs due to the Pt sites released from the oxidation/desorption of acetylene. These results indicate the dependence of the cell performance loss on the acetylene concentration at low concentration levels. Below a certain concentration, the acetylene adsorption and oxidation equilibrated, and the acetylene was oxidized completely without intermediate accumulation.

3.2.2. Contamination at different cell current densities

During the acetylene contamination tests under different current densities, the impedance spectra were measured at the pre-poisoning and steady poisoning states (if a steady state was reached). It should be noted that only the EIS obtained under steady states were reliable [31]. For example, in Fig. 2 b), the test at 1.5 A cm^{-2} with 200 ppm acetylene did not reach a steady poisoning state until recovery. Reliable EIS were not available for this study. Therefore, the EIS obtained from the experiments at 0.2 and 0.6 A cm^{-2} with 300 ppm acetylene in Fig. 2 c) were selected to demonstrate the significant current density effects, as shown in Fig. 5 a). The EIS of the quasi-steady poisoning state at 0.6 A cm^{-2} is also included. Before exposure to acetylene, the MEAs showed their typical EIS at low and high current densities, respectively, with three distinguishable depressed semicircles. The mid-frequency semicircles at 0.2 A cm^{-2} are much bigger than those at 0.6 A cm^{-2}, indicating the higher ORR resistance at a lower current density [32]. The overpotential at a low current density was much lower than that at a high current density. When the cell was exposed to 300 ppm acetylene, at 0.2 A cm^{-2}, only the mid-frequency arc of the EIS in the steady poisoning state was slightly expanded compared to that before exposure, but the low frequency arc did not change obviously. The change in the mid-frequency arc suggested the low coverage of acetylene on the cathode, which slightly affected the ORR without affecting the mass transport of oxygen in the MEA. For the exposure at 0.6 A cm^{-2}, the EIS at the quasi-steady poisoning state, i.e., after 0.5 h of exposure, shows obviously expanded arcs in the mid and low frequencies; when the cell performance reached the steady poisoning state, the mid and low frequency arcs were significantly enlarged, and an inductive arc was observed. These features are similar to those of the steady poisoning state at 1 A cm^{-2}, which were discussed in Fig. 4 a). However, the expansions of the mid and low frequency arcs at the steady poisoning state at 0.6 A cm^{-2} are much smaller than those at 1 A cm^{-2}. These results indicate that at a cathode potential above the acetylene reduction potential, the acetylene poisoning was more severe at a high current density than at a low current density due to the potential dependency of the acetylene oxidation. In contrast, when the cathode potential became lower than the acetylene reduction potential, the acetylene poisoning became more severe at a low current density than at a high current density due to the potential dependency of the acetylene reduction.

For the current density effect, the ECM was applied to the EIS obtained during the 100 ppm acetylene experiments at 0.2, 0.6 and 1 A cm^{-2} in Fig. 2 a). As mentioned in section *3.2.1*, obvious changes in R or Ra were not observed. The Rc and Rd data fits are shown in Fig. 5 b). Before exposure, the ORR charge resistance, Rc, was constant at 0.248, 0.125 and 0.107 Ω cm^2, and the mass transfer resistance Rd were constant at 0.075, 0.056 and 0.061 Ω cm^2 for the current densities of 0.2, 0.6 and 1 A cm^{-2}, respectively. The initial ORR charge resistance decreased with increase in the cell current density due to the higher overpotential for the ORR at a high current density than that at a low current density [32,33]. At the steady poisoning state, the Rc increased to approximately 0.253, 0.129 and 0.112 Ω cm^2, and Rd increased to 0.080, 0.061 and 0.064 Ω cm^2, respectively. The Rc increased by 2.0%, 3.2% and 4.7% and the Rd increased by 6.7%, 8.9% and 4.9% for the current densities of 0.2, 0.6 and 1 A cm^{-2}, respectively. The increases in Rc and Rd corresponded to the competition between the acetylene oxidation on the Pt and the ORR and accounted for the cell performance losses during acetylene contamination at different current densities. Additionally, the poisoning impact of acetylene on the ORR increased with the increase in the operating current density. According to the acetylene contamination mechanisms, the adsorbed acetylene could be oxidized at potentials above 0.65 V [24]. The cathode potentials at those three current densities were all above 0.65 V. However, the cell cathode potential was higher at a low current density than that at a high

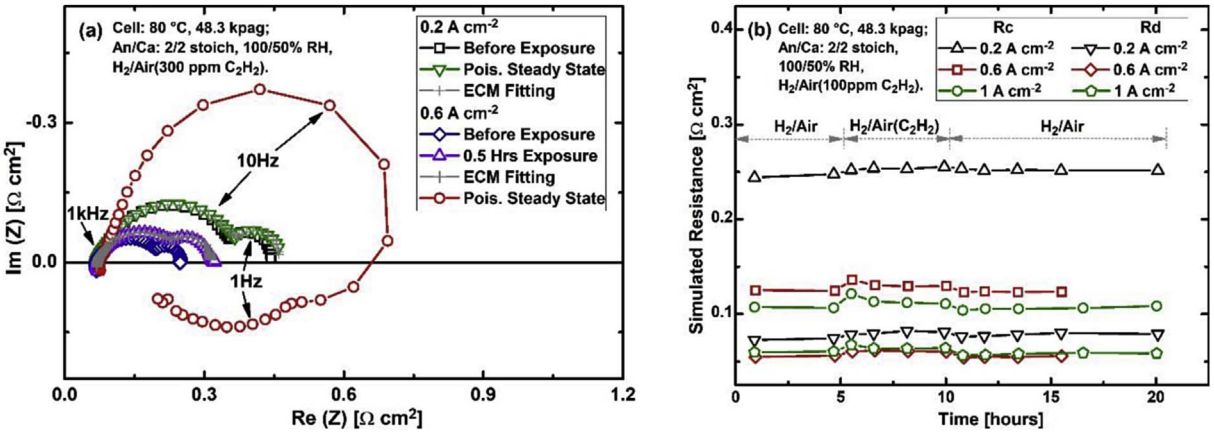

Fig. 5. a) EIS of the MEAs during the acetylene contamination experiments with different current densities at 80 °C and b) the variations in the Rc and Rd during the acetylene contamination experiments. (For interpretation of the references to colour in this figure legend, the reader is referred to the web version of this article.)

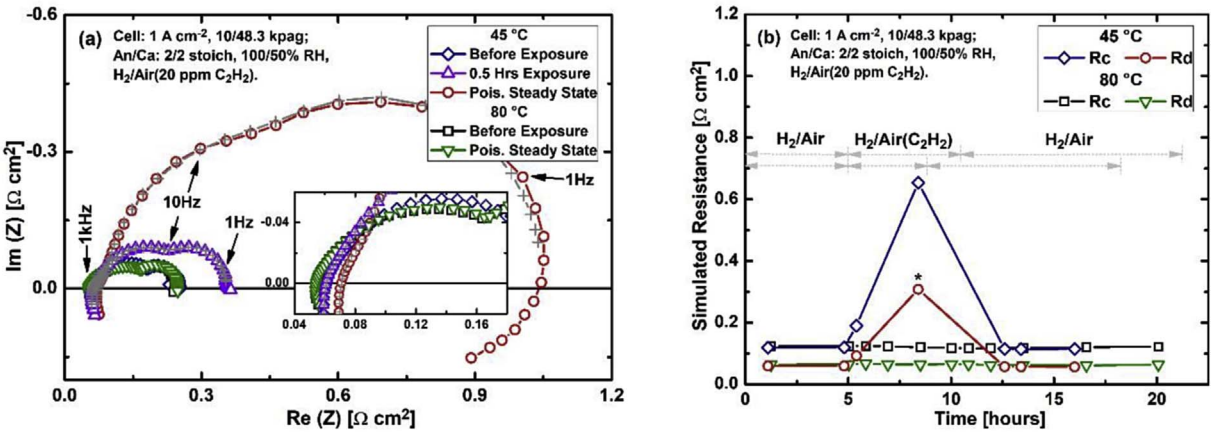

Fig. 6. a) EIS of the MEAs during the 20 ppm acetylene contamination experiments with a current density of 1 A cm^{-2} at 80 °C or 45 °C. The inset is a magnification of the high frequency region. b) The variations in Rc and Rd during the 20 ppm acetylene contamination experiments. (For interpretation of the references to colour in this figure legend, the reader is referred to the web version of this article.)

current density, resulting in a higher overpotential for the oxidation of acetylene on the cathode. After recovery, the Rc and Rd values for both MEAs returned to their initial values due to the Pt sites released during the oxidation desorption of acetylene.

3.2.3. Cell temperature effect

Regarding the effect of the cell operating temperature, the high concentration (100 ppm) acetylene contamination tests did not reach a steady poisoning state under low temperature, as shown Fig. 3 a). Therefore, the EIS obtained during the 20 ppm acetylene contamination tests (Fig. 3) b) at 80 and 45 °C are shown in Fig. 6 a) with magnifications of the high-frequency arcs in the inset. The inset indicates that before exposure, the MEAs at 45 and 80 °C had membrane proton transfer resistances of 0.060 and 0.054 Ω cm^2, respectively (high frequency intercepts with the real impedance axis). The mid-frequency arc at 45 °C shows a slightly bigger diameter than that at 80 °C, which indicates a slightly higher ORR resistance. Generally, at low temperatures, the MEA exhibited a low proton conductivity due to the low water content and a high ORR resistance due to the slow reaction kinetics. During exposure to 20 ppm acetylene at 80 °C, the EIS within all frequency ranges overlapped with that obtained before exposure. However, for exposure at 45 °C, 0.5 h of acetylene exposure caused obvious enlargement in the mid- and low-frequency arcs. When the acetylene poisoning reached the steady state, as indicated in Fig. 6 a), both the mid- and low-frequency arcs were significantly expanded. In addition, parts of an inductive loop also appeared. It should be noted that the high frequency intercept was also shifted to a high resistance value of 0.071 Ω cm^2 because the cell temperature control was lost, leading to an increase to 55 °C without and adjustment to the humidifier temperature.

The ECM was applied to the EIS obtained during the 20 ppm acetylene experiments at 80 and 45 °C. The Rc and Rd fitting results are shown in Fig. 6 b). Before acetylene exposure, both Rc and Rd were similar at 80 and 45 °C, at approximately 0.12 and 0.062 Ω cm^2, respectively. During exposure at 80 °C, both Rc and Rd remained constant, but significant increases occurred in both Rc and Rd at 45 °C. During exposure at 45 °C, after approximately 0.5 h, a quasi-steady poisoning state was achieved, as shown in Fig. 3 b). In this first stage, Rc and Rd increased approximately 58.3% and 17.7% to 0.19 and 0.073 Ω cm^2, respectively; when the cell reached the steady poisoning state, Rc and Rd increased to 0.65 and 0.308 Ω cm^2, respectively. These resistances constituted a 440% increase in Rc and a 400% increase in Rd over their initial values. When the acetylene exposure was stopped, both of the resistances returned to their initial values. For the exposure at 80 °C, the cathode potential and cell temperature were sufficiently high to facilitate a high reaction rate to completely oxidize the 20 ppm acetylene without obvious effects on the ORR. In contrast, the significant increases in Rc and Rd at 45 °C accounted for the slow oxidation and strong adsorption of acetylene and/or CO/COH-type intermediates [27–29]. These adsorbates competed with the ORR on the Pt and affected the large cell performance losses during the acetylene contamination. These results indicate that the acetylene contamination severely depends on the cell temperature; a stronger poisoning effect on the ORR charge transfer and mass transport processes occurred at lower cell temperatures.

3.3. MEA polarization curves

Before and after all contamination experiments, the cell polarization curves were collected from 2 A cm^{-2} to the OCV to determine the permanent effects of acetylene contamination on the cell performance. Fig. 7 shows the polarization curves before and after the acetylene contamination experiments with different concentrations of acetylene in the cathode under different current densities or at different cell temperatures. From Fig. 7 a) and b), all the polarization curves of the MEAs after exposure to different concentrations of acetylene and at different current densities completely overlapped with those obtained before exposure. This result indicates that no activation, ohmic polarization or mass transport effect remains on the MEAs after neat air operation, indicating complete performance recovery. From Fig. 7 c), for the cell at 45 °C, the cell performance was improved after the acetylene contamination test, especially for the cell current density above 1 A cm^{-2}. However, for the cell at 10 °C, the cell performance was reduced slightly after the acetylene contamination test, and the cell voltage decreased further when the cell current density was higher than 0.8 A cm^{-2}. These results agree well with the cell voltage changes during constant-current operation and imply that mass transport may impact acetylene contamination on the MEA catalyst layers. The reason is not clear yet and requires further investigation.

3.4. Proposed acetylene contamination mitigation strategy

The single cell could be considered as a plug-flow electrochemical reactor. The electrochemical and catalytic reaction rates of the acetylene positively depended on the acetylene concentration, the effective active area of the electrode and the cell cathode potential. The contamination overpotential, i.e., the cell performance loss, positively depended on the coverage of acetylene and other intermediate adsorbates on the electrode surface. The cathodes with higher potentials facilitated the acetylene oxidation and diminished the accumulation of the adsorbates on the cathode; the cathodes with lower potentials enhanced the acetylene reduction and removed the acetylene adsorbates more

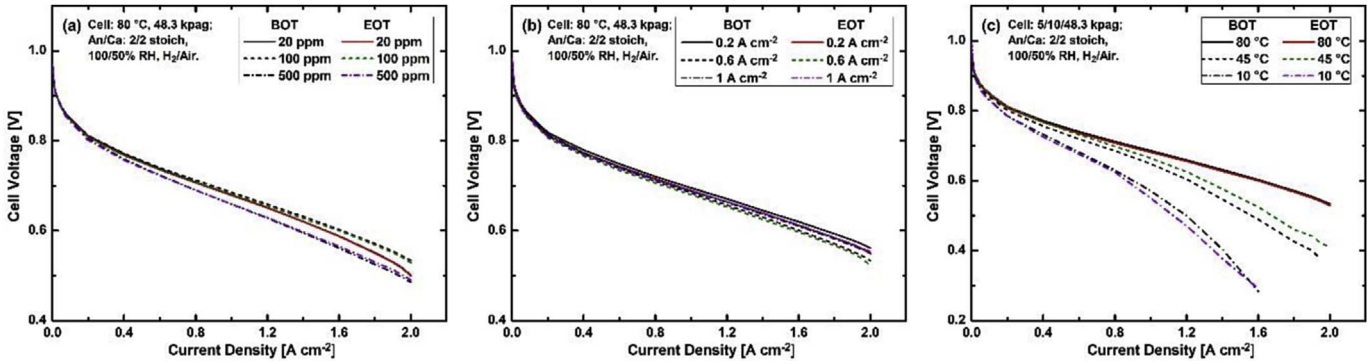

Fig. 7. Cell polarization curves before and after acetylene contamination experiments a) with different concentrations at 80 °C and 1 A cm^{-2}, b) under different current densities at 80 °C with 300 ppm acetylene, or c) at different cell temperatures at 1 A cm^{-2} with 100 ppm acetylene. (For interpretation of the references to colour in this figure legend, the reader is referred to the web version of this article.)

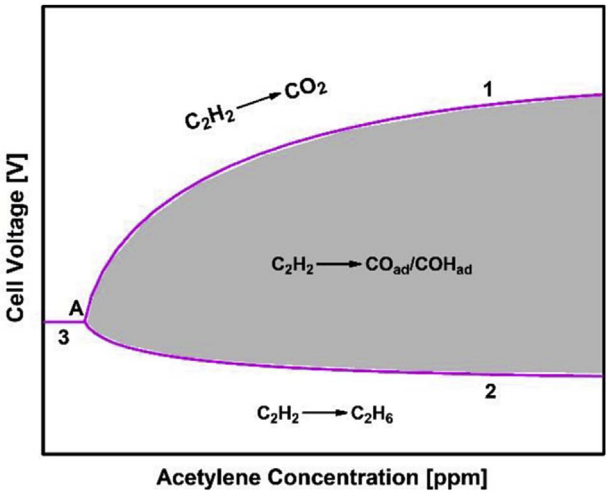

Fig. 8. Illustration of the dependency of the acetylene contamination on the acetylene concentration and the cell cathode potential.

readily. These results suggest that concentration and potential barriers existed. Both parameters interacted with each other, depending on the cell temperature, and limited the tolerance of the PEMFC to acetylene. As illustrated in Fig. 8, there is an acetylene oxidation equilibrium line (line 1), an acetylene reduction equilibrium line (line 2), an intersection A where lines 1 and 2 meet, and a boundary between oxidation and reduction regions (line 3). Above lines 3 and 1, the acetylene and the intermediates could be completely oxidized into CO_2 and desorbed; below lines 3 and 2, the acetylene could be completely reduced and desorbed. However, in the gray area between lines 1 and line 2, the acetylene adsorbates or the intermediates could not completely oxidize or reduce. Under the conditions within the gray area, the adsorbate or intermediate accumulation would cause severe cell performance losses. If a cell is operated with an acetylene concentration below point A, severe cell performance losses from acetylene contamination should not occur. If the cell is contaminated with a high concentration of acetylene, similar to the conditions in the gray area, the effect on the cell performance may be eliminated by changing the cell voltage.

4. Conclusion

The contamination effect of acetylene in PEMFCs significantly depended on the cell temperature, cathode potential, and acetylene concentration. Low concentrations of acetylene in the air slightly impacted the cell performance due to the low coverage of acetylene adsorbates caused by the complete oxidation at high cell voltages. Higher concentrations of acetylene in the air stream caused increased cell performance losses due to the accumulation of adsorbates and CO and/or COH-type intermediates on the cathode. The poisoning became more severe at medium cell current densities. The cell cathode potentials at these current densities were not sufficiently high to completely oxidize the intermediates or sufficiently low to completely reduce the adsorbed acetylene. Higher cell temperatures reduced the acetylene poisoning effect due to enhanced the oxidation and reduction of acetylene on the cathode. Concentration and potential barriers may exist, and both parameters interacted with each other, depending on the cell temperature, to determine the tolerance limit of the PEMFC to acetylene. For the GORE PRIMEA M715 MEA with 0.4/0.4 mgPt cm^{-2} in cathode/anode, the threshold concentrations (5-20 ppm at 45 °C, 200-300 ppm at 80 °C) exceed the 3–5.5 ppm concentration in ambient air near acetylene production plants. Moreover, for PEMFC operation in the field with ambient air, a significant performance loss is not expected. However, if severe contamination does occur under unusual conditions, such as a faulty or saturated intake filter coupled with an ambient temperature startup or sudden and localized release from an acetylene cylinder, the cell operation parameters can be adjusted to reverse it by inducing complete acetylene oxidation or reduction.

Acknowledgments

The authors are indebted to the United States Department of Energy for funding (award DE-EE0000467) and the Office of Naval Research (award N00014-12-1-0496). The authors are grateful to the Hawaiian Electric Company for their ongoing support to the operations of the Hawaii Sustainable Energy Research Facility.

References

[1] M.K. Debe, Nature 486 (2012) 43–45.
[2] R. Borup, et al., Chem. Rev. 107 (2007) 3904–3951.
[3] http://www.epa.gov/airquality/airdata/index.html.
[4] J. St-Pierre, F.N. Büchi, M. Inaba, T.J. Schmidt (Eds.), Polymer Electrolyte Fuel Cell Durability, Springer, New York, 2009, pp. 289–321.
[5] X. Cheng, Z. Shi, N. Glass, L. Zhang, D. Song, Z. Liu, H. Wang, J. Shen, J. Power Sources 165 (2007) 739–756.
[6] Z. Ma, F. Zaera, Surf. Sci. Rep. 61 (2006) 229–281.
[7] J.M. Moore, P.L. Adcock, J.B. Lakeman, G.O. Mepsted, J. Power Sources 85 (2000) 254–260.
[8] Y. Garsany, O.A. Baturin, K.E. Swider-Lyons, J. Electrochem. Soc. 154 (2007) B670–B675.
[9] R. Mohtadi, W.K. Lee, J.W. Van Zee, J. Power Sources 138 (2004) 216–225.
[10] F. Jing, M. Hou, W. Shi, J. Fu, H. Yu, P. Ming, B. Yi, J. Power Sources 166 (2007) 172–176.
[11] Y. Nagahara, S. Sugawara, K. Shinohara, J. Power Sources 182 (2008) 422–428.
[12] H. Li, H. Wang, W. Qian, S. Zhang, S. Wessel, T. Cheng, J. Shen, S. Wu, J. Power Sources 196 (2011) 6249–6255.
[13] O.A. Baturina, A. Epshteyn, P.A. Northrup, Karen E. Swider-Lyons, J. Electrochem. Soc. 158 (2011) B1198–B1205.
[14] W. Yan, H. Chu, Y. Liu, F. Chen, J. Jang, Int. J. Hydrogen Energy 36 (2011) 5435–5441.

[15] S. Ali, Q. Li, C. Pan, J. Jensen, L. Nielsen, P. Møller, Int. J. Hydrogen Energy 36 (2011) 1628–1636.
[16] H. Li, J. Zhang, Z. Shi, et al., J. Electrochem. Soc. 156 (2009) B252–B257.
[17] M. Smith, D. Myers, 211th ECS meeting, Abs.0214.
[18] Y. Zhai, G. Bender, S. Dorn, R. Rocheleau, J. Electrochem. Soc. 157 (2010) B20–B26.
[19] S. Dorn, Y. Zhai, R. Rocheleau, ECS Trans. 28 (23) (2010) 183–191.
[20] J. St-Pierre, Y. Zhai, M. Angelo, J. Electrochem. Soc. 161 (3) (2014) F280–F290.
[21] R. Patterson, M. Bornstein, E. Garshick, Assessment of Acetylene [etc.] as a Potential Air Pollution Problem: Final Report, for U.S. Environmental Protection Agency, GCA Corporation, Technology Division, 1976.
[22] Y. Zhai, J. St-Pierre, J. Power Sources 279 (2015) 165–171.
[23] J. Ge, J. St-Pierre, Y. Zhai, Electrochimica Acta 133 (2014) 65–72.
[24] Y. Zhai, J. St-Pierre, Chem. Electro. Chem 4 (2017) 655–670.
[25] J. St-Pierre, Y. Zhai, M. Angelo, Int. J. Hydrogen Energy 37 (2012) 6784–6789.
[26] T.V. Reshetenko, J. St-Pierre, J. Power Sources 287 (2015) 401–415.
[27] S. Balasubramanian, B. Lakshmanan, C.E. Hetzke, V.A. Sethuraman, J.W. Weidner, Electrochimica Acta 58 (2011) 723–728.
[28] F. Maillard, E. Savinova, U. Stimming, J. Electroanal. Chem. 599 (2007) 221–232.
[29] M. Byrne, A. Kuhn, V. Whittle, J. Chem. Soc. Faraday Trans. 1 (69) (1973) 787–793.
[30] C.E. Megiris, P. Berlowitz, J. Butt, H. Kung, Surf. Sci. 159 (1) (1985) 184–198.
[31] Y. Zhai, K. Bethune, G. Bender, R. Rocheleau, J. Electrochem. Soc. 159 (2012) B524–B530.
[32] M. Kumagaia, S. Myung, T. Ichikawab, H. Yashiro, J. Power Sources 195 (2010) 5501–5507.
[33] M. Ciureanu, R. Roberge, J. Phys. Chem. B 105 (2001) 3531–3539.